



LHC BFPP Quench Test with Ions (2015)

R. Alemany, B. Auchmann, C. Bahamonde Castro, V. Chetvertkova,
R. Giachino, J.M. Jowett, M. Kalliokoski, A. Lechner, T. Mertens, L. Ponce,
M. Schaumann
CERN, CH-1211 Geneva 23

Keywords: LHC, Heavy Ion, BFPP, Quench Test

Summary

The 2015 Pb-Pb collision run of the LHC operated at a beam energy of 6.37Z TeV. The power of the secondary beams emitted from the interaction point by the bound-free pair production (BFPP) process reached new levels while the propensity of the bending magnets to quench is higher at the new magnetic field levels. This beam power is about 70 times greater than that contained in the luminosity debris and is focussed on a specific location. As long foreseen [1, 2, 3], orbit bumps were introduced in the dispersion suppressors around the highest luminosity experiments to mitigate the risk of quenching by displacing and spreading out these losses.

Because the power of these secondary beams is well known and the loss location can be easily determined with Beam Loss Monitors (BLMs), the BFPP1 beam ($^{208}\text{Pb}^{81+}$ ions), which is the most intense, provides a tool to accurately deduce the steady state quench limit of the LHC main dipoles [4]. At the moment the exact quench limit is not known, but this knowledge is important for LHC operation (e.g. setting BLM thresholds) and to assess the need for special collimators to intercept these secondary beams.

This note describes the procedure and preliminary results of a test conducted on the main dipole in cell 11 left of IP5, using the BFPP1 beam to provoke a quench of this magnet.

Contents

1	Introduction	2
1.1	Secondary Beams from Luminosity Production	2
1.2	Orbit Bump Technique	3
1.3	Potential for Quench Test	4
2	Requirements and Preparation	4

3	Conducting the Experiment	6
3.1	Initial Setup as for Standard Physics Fill	6
3.2	Specific Actions for the Quench Test	8
4	Preliminary analysis with FLUKA	13
5	Summary and Conclusions	15

List of Figures

1	Example of BFPP trajectory right of IP5.	3
2	Zoom to impact location of the BFPP beam right of IP5.	4
3	Orbit bumps of Beam 2 around cell 11 left of IP5.	5
4	Initial beam parameters.	7
5	Beam intensity evolution from injection to beam dump.	7
6	Loss patterns around IP5.	9
7	BLM signals with different bump amplitudes.	10
8	Preliminary FLUKA simulations used for bump optimization.	10
9	Luminosity evolution.	11
10	BLM signal evolution.	11
11	Beam parameters before quench.	12
12	Quench detection - Voltage difference across the two magnet apertures.	13
13	BLM signal comparison between experimental data from the quench test and FLUKA data.	14
14	Peak power density in the MB.B11L5 coils during the quench test estimated by FLUKA simulations.	15

List of Tables

1	Average beam parameters during the experiment.	8
---	--	---

1 Introduction

1.1 Secondary Beams from Luminosity Production

In the collision of two fully stripped ions ultraperipheral electromagnetic interactions dominate the total cross-section. The most important interaction in Pb collisions is the Bound-Free Pair Production (BFPP):



where in the first order reaction ($n = 1$, BFPP1) one of the participating ions captures an electron. These reactions change the charge state of one of the colliding ions and thus its magnetic rigidity, creating secondary beams emerging from the collision point. The secondary beams will follow dispersive orbits according to their magnetic rigidity. However their effective momentum

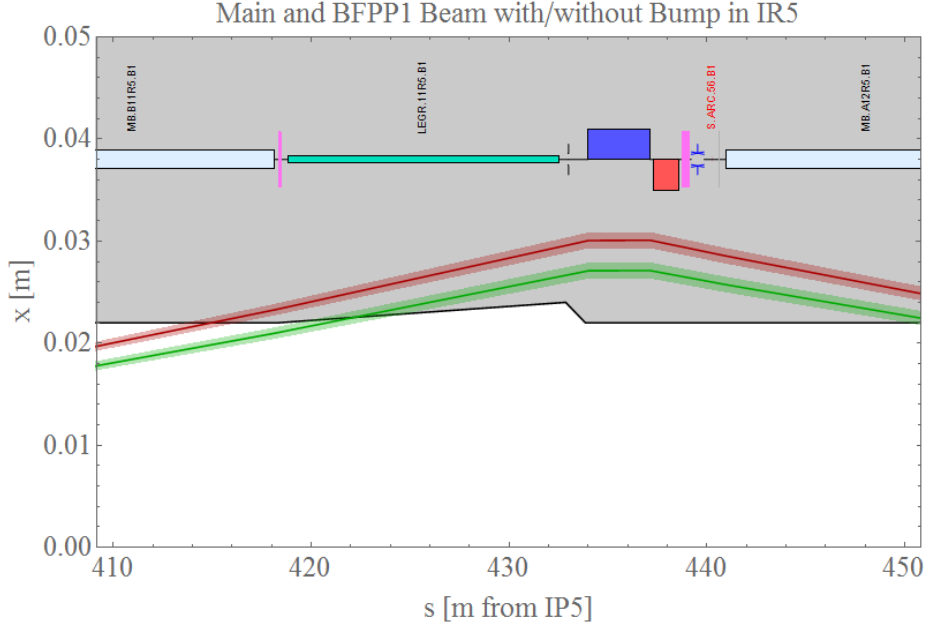


Figure 2: Zoom into Fig. 1 to impact location of the BFPP beam right of IP5. Red trajectory calculated without orbit bump, green with a bump amplitude of -3 mm at Q11.

1.3 Potential for Quench Test

Using the BFPP1 beam to induce a quench has the advantage that the impact point in the magnet can be controlled by modifying the orbit bumps, so that quenches at the end of the magnet, which would return less accurate estimates for the quench limits due to the specifics of the magnet design, can be avoided. Another advantage is that the power in the BFPP beam is directly dependent on the luminosity at the interaction point, which can also be controlled by changing the beam separation at the interaction point considered. This method can therefore provide a very clean loss scenario, that can be reconstructed with FLUKA [6, 7] simulations. By scaling the FLUKA results to the achieved Pb-Pb luminosity, one can derive an estimate of the peak power density leading to a quench.

2 Requirements and Preparation

As the presently known quench limit is affected with some error, a physics fill with as high as possible luminosity is required for the experiment in order to achieve high enough loss rates to potentially induce a quench. Therefore the test was performed close to the end of the ion run (on 8 December 2015) when the highest available intensity and lowest transverse emittance were available in the LHC.

The detailed description of the procedure for changing BLM thresholds for this MD is described in Ref. [8]. The modified thresholds should allow the dipole magnets in the dispersion suppressors to quench and also avoid unwanted beam dumps before this regime of losses is reached. As changes of BLM thresholds or monitoring factors are not possible during the fill, the changes have to be applied before the fill intended to perform the BFPP quench test, and have to be undone during

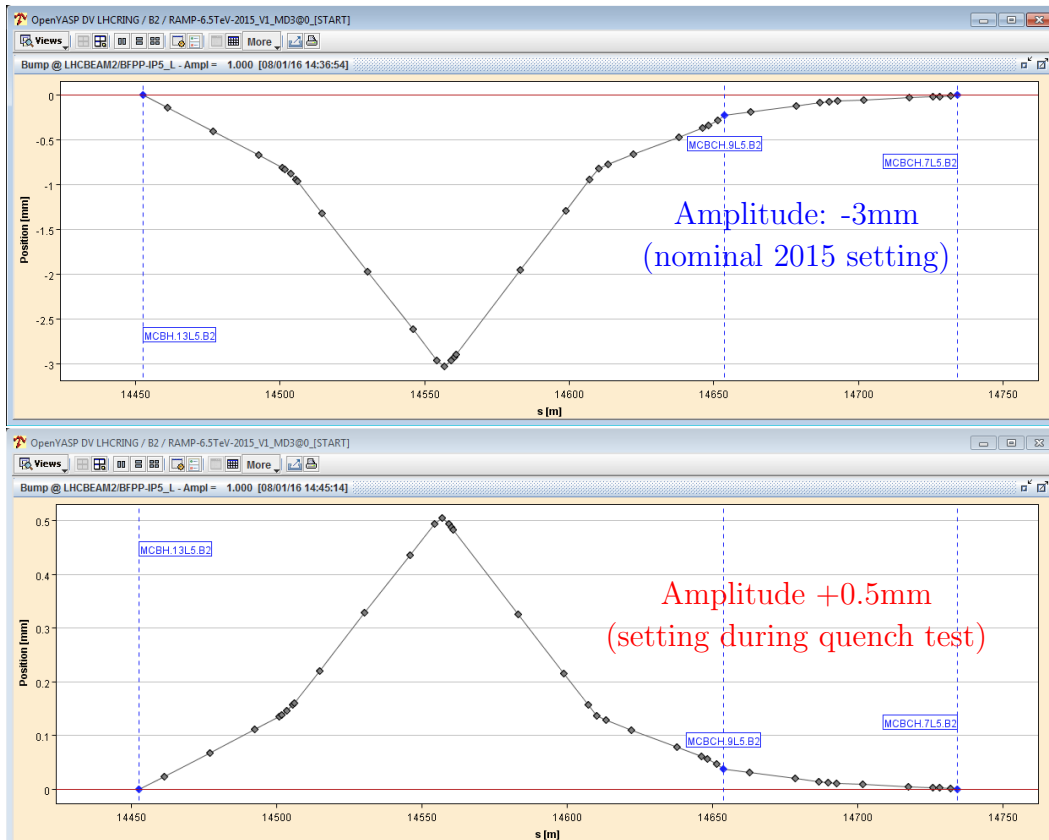


Figure 3: Orbit bump of Beam 2 around cell 11 left of IP5 with a maximum amplitude of -3 mm (top, maximum with loss maps validated amplitude for operation in 2015) and $+0.5$ mm (bottom, as used during the quench test, amplitude chosen from observed BLM signals before the test).

ramp-down after the end of the test.

Following the initial commissioning and operation for physics before the experiment, the BFPP bumps around IP1, IP2 and IP5 were all set to the validated maximum values, corresponding to a peak radial displacement of the orbit of -3 mm. A comparison of the measured losses on BLMs with the FLUKA simulation performed earlier confirmed the loss locations:

- IP1: losses are in the connection cryostat on both right and left of the IP.
- IP2: the BFPP losses on the right side were (partially) moved into the dipole MB.C12R2 beyond the connection cryostat and were somewhat more spread out than they would be without the bump. On the left side, the bump was not large enough to move the losses from cell 10 to 12.
- IP5: On the right, the situation is similar to IP1. On the left, it appears that the BFPP bump was insufficient to move the losses completely into the connection cryostat. A test with a bump some 2 mm larger (total amplitude -5 mm) appeared to achieve this. The maximum losses were moved into the interconnection. This is attributed either to a closed orbit displaced towards the outside of the ring (by roughly 2 mm) in this location or a misalignment of the beam screen in the opposite direction. Some losses were also observed here even before the beams collided.

The luminosity at CMS and ATLAS rose to values around $1.8 \times 10^{27} \text{ cm}^{-2}\text{s}^{-1}$.

According to the observed loss situation, the location left of IP5 was chosen for the experiment, because here the beam impact position lies deep inside the dipole without orbit bump, which is required for a clean measurement of the quench limit. In the other IPs, the beams would impact close to the end of the dipole or in the interconnect without orbit bump, which is an undesired location for the test. The BFPP loss location in the chosen magnet can be determined from FLUKA simulations by comparing simulated and measured BLM patterns.

3 Conducting the Experiment

In this section the actions performed during the experiment are listed in order of execution. Moreover, the initial beam conditions at injection and just before starting the test are presented.

3.1 Initial Setup as for Standard Physics Fill

The LHC was filled with the highest possible intensity and as low as possible emittances, as during a standard physics fill. The average beam parameters are listed in Table 1. Filling started around 19:00, in Fill number 4707. The initial bunch intensities (left), bunch length (right) are shown in Fig. 4. The evolution of the beam intensity through injection until the beams were dumped is shown in Fig. 5.

After the ramp to $6.37 Z$ TeV, the pre-squeeze of ALICE, main squeeze of all IPs down to $\beta^* = 0.8$ cm, the collision preparation beam process (ALICE crossing angle adjustment and IP displacement) and the collision beam process (to correctly play the collimator functions for validated machine protection setup) were performed as for physics. Collisions started around 20:40.

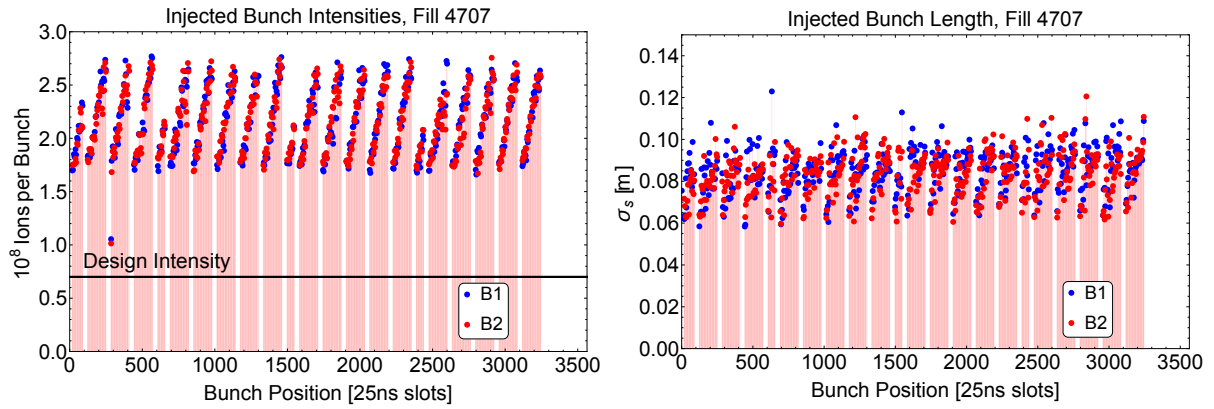


Figure 4: Initial beam parameters of Fill 4707. Bunch intensities (left), bunch length (right); blue displays Beam 1, red Beam 2.

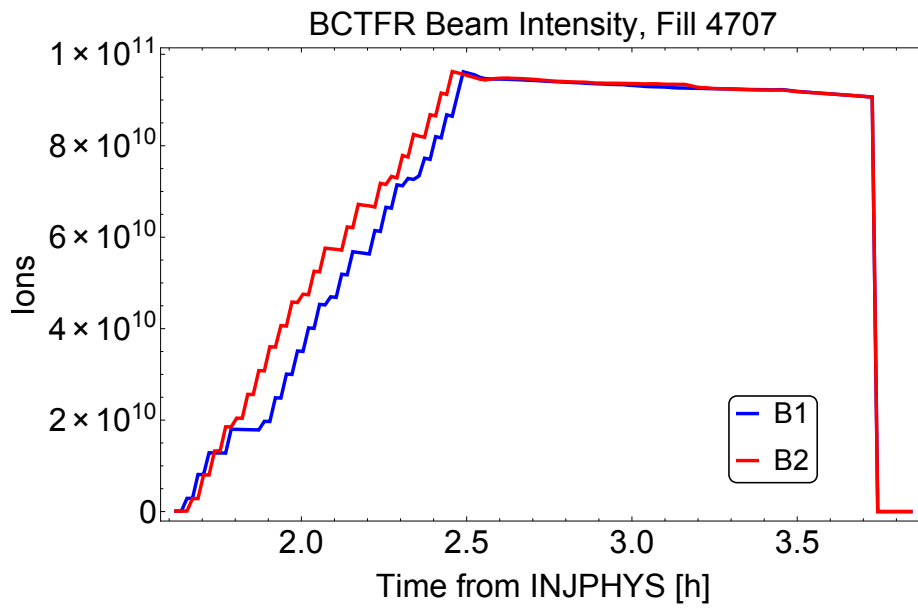


Figure 5: Beam intensity evolution from injection to beam dump.

Fill number	4707
Injection	
Injected bunch intensity [10^8 ions]	2.2 ± 0.3
Injected bunch length [m]	0.084 ± 0.010
Before Dump at Top Energy	
Bunch intensity before dump [10^8 ions]	1.9 ± 0.3
Bunch length before dump [m]	0.092 ± 0.003
Horizontal normalised emittance, B1 [μm]	2.2 ± 0.2
Horizontal normalised emittance, B2 [μm]	2.0 ± 0.2
Vertical normalised emittance, B1 [μm]	1.2 ± 0.2
Vertical normalised emittance, B2 [μm]	1.7 ± 0.2

Table 1: Average beam parameters during the experiment.

3.2 Specific Actions for the Quench Test

From this point on, we departed from the nominal sequence in order to perform actions specific to the experiment.

- Continue in ADJUST beam mode.
- Separate all IPs in order reduce burn-off and save peak luminosity to achieve the highest BFPP beam intensity.
- Luminosity optimisation with subsequent re-separation in one plane for IP1 and 5 to ensure the beam centres are not too far off and that we arrive head on in IP5 when colliding in steps.

This was only the second fill with the given configuration and the beam positions with respect to the collimators were not yet optimised.

- Reduce the beam separation at IP5 to have enough luminosity available to determine the impact point of the BFPP beam in the bending magnet based on BLM signals and comparison with FLUKA simulations.
- Reduce the BFPP orbit bumps left of IP5 to zero, until it is clear that the loss location has moved into the body of the MB.

The original bump amplitude was -3 mm.

We set the amplitude to $+0.5$ mm for the experiment.

Figure 6 shows the initial loss situation around IP5, a zoom to the left side is shown in Fig. 7 with an orbit bump of -3 mm (red) and $+0.5$ mm (blue). The shift of the loss peak deep into the MB is clearly visible.

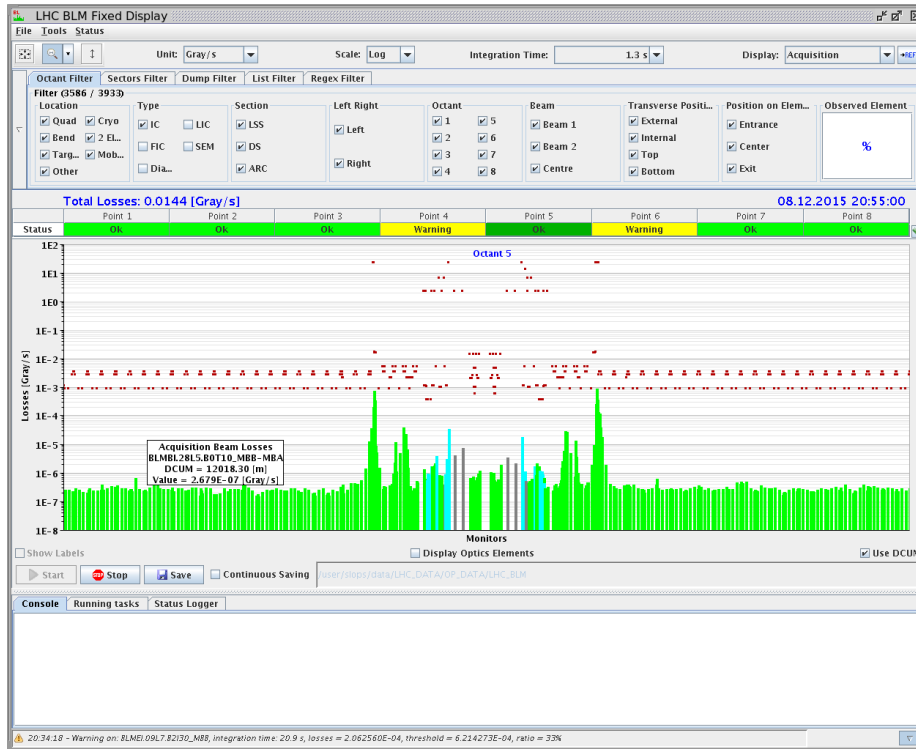


Figure 6: Loss patterns around IP5.

The observed loss pattern was compared to FLUKA simulations shown in Fig. 8 in order to estimate the impact position from the BLM signals and optimize the bump amplitude used for the experiment.

- Reduce the beam separation at IP5 to zero in steps of $5 \mu\text{m}$, wait a few minutes between each step for the conditions to stabilize.

Start decreasing separation around 21:00.

The luminosity in CMS and BLM signal evolution during the experiment is shown in Fig. 9 and 10, respectively.

After performing the 4th step and arriving at the head on position, a quench occurred (21:07) at an instantaneous luminosity of $\mathcal{L} \approx 2.3 \times 10^{27} \text{ cm}^{-2}\text{s}^{-1}$ in CMS. If the BFPP beam intensity had not been enough to provoke the quench, we could still have performed a luminosity optimisation. The beam conditions just before the beam dump are shown in Fig. 11 and the average conditions are summarized in Table 1.

A look at the post mortem files revealed that a real quench occurred. In Fig. 12 the voltage difference across the two (Beam 1 and 2) magnet apertures is shown in blue. The rise of this voltage over a few milliseconds is a clear sign of a quench in one of the two apertures. When it reaches 250 mV the quench heaters are triggered, leading to a quench of the second aperture within a few milliseconds delay from the first.

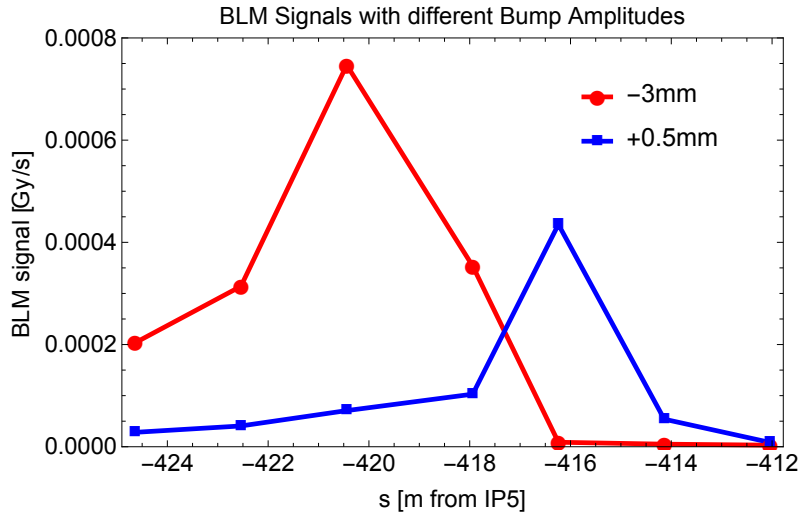


Figure 7: BLM signals of running sum 9 (1.3 s) for the orbit bump amplitude of -3 mm around 3.5 h (see time scale in Fig. 10) and $+0.5$ mm before increasing the luminosity (around 3.67 h). IP5 is placed on the right side of the plot at $s = 0$ m. The beam is propagating from right to left in this figure.

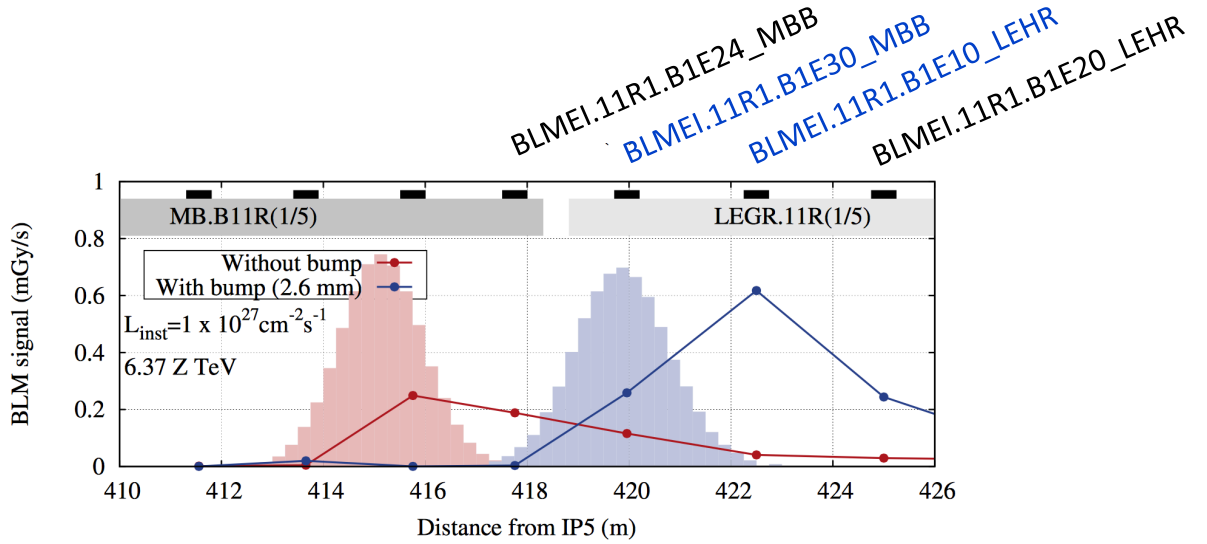


Figure 8: Preliminary FLUKA simulation of the BLM signals in cell 11 right of IP5, performed with an orbit bump of -2.6 mm (blue) and 0 mm (red). The beam travels from the left to the right side of the plot. The situation to the left side of the IP is expected to be similar.

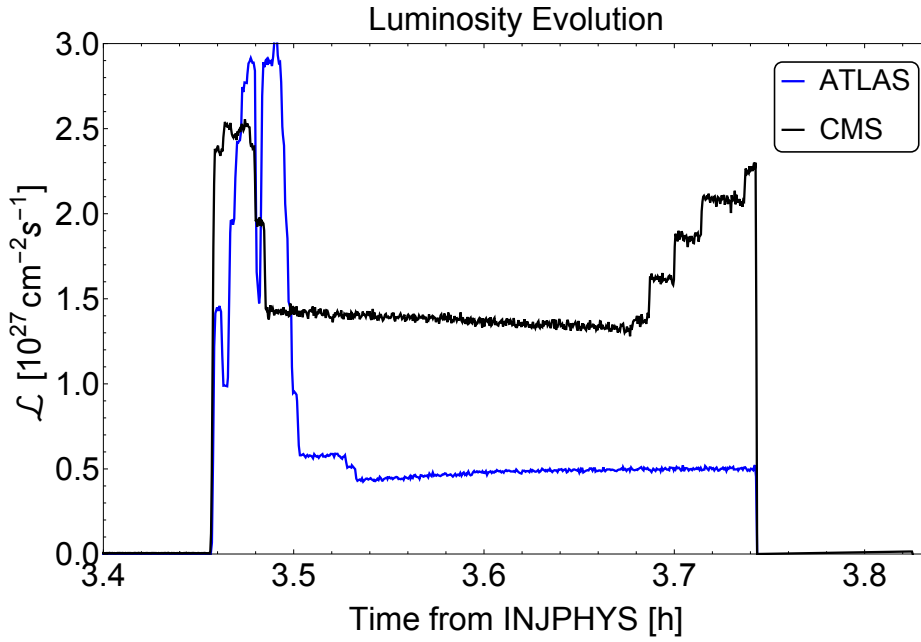


Figure 9: Luminosity evolution in CMS and ATLAS during the experiment. A quench occurred after increasing the CMS luminosity for the 4th time and the beam was dumped.

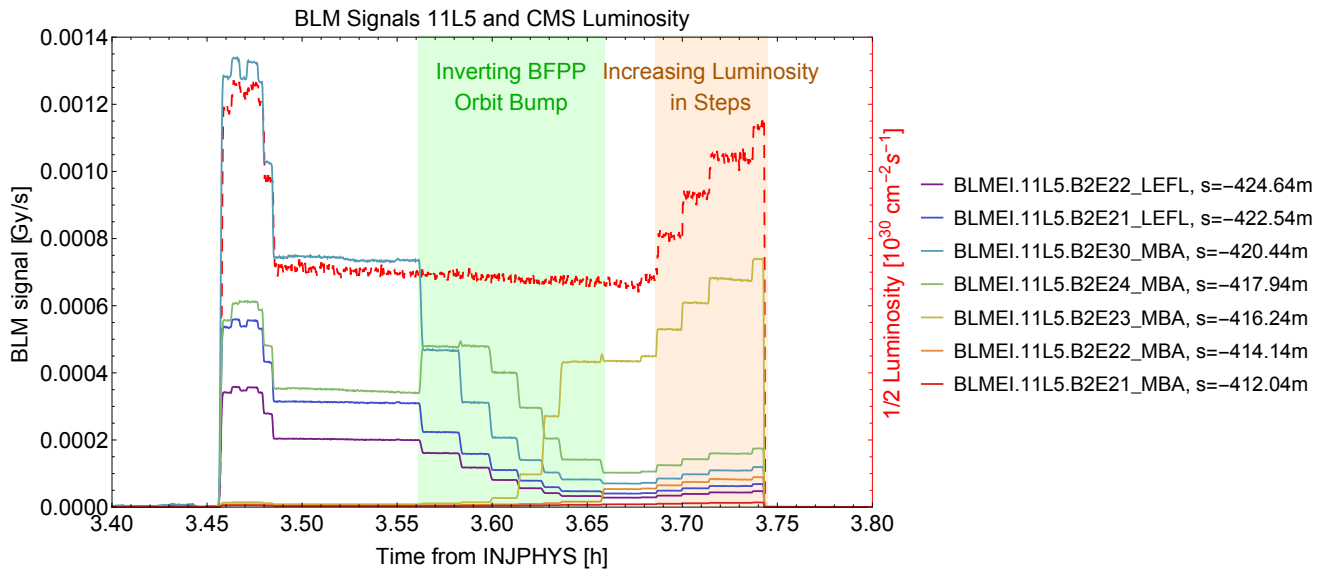


Figure 10: BLM signals of running sum 9 (1.3s) and CMS luminosity (red dashed line, divided by 2 to fit the scale) during the quench test. The period while the orbit bump was inverted is highlighted in green, the increase of the luminosity until the quench in orange.

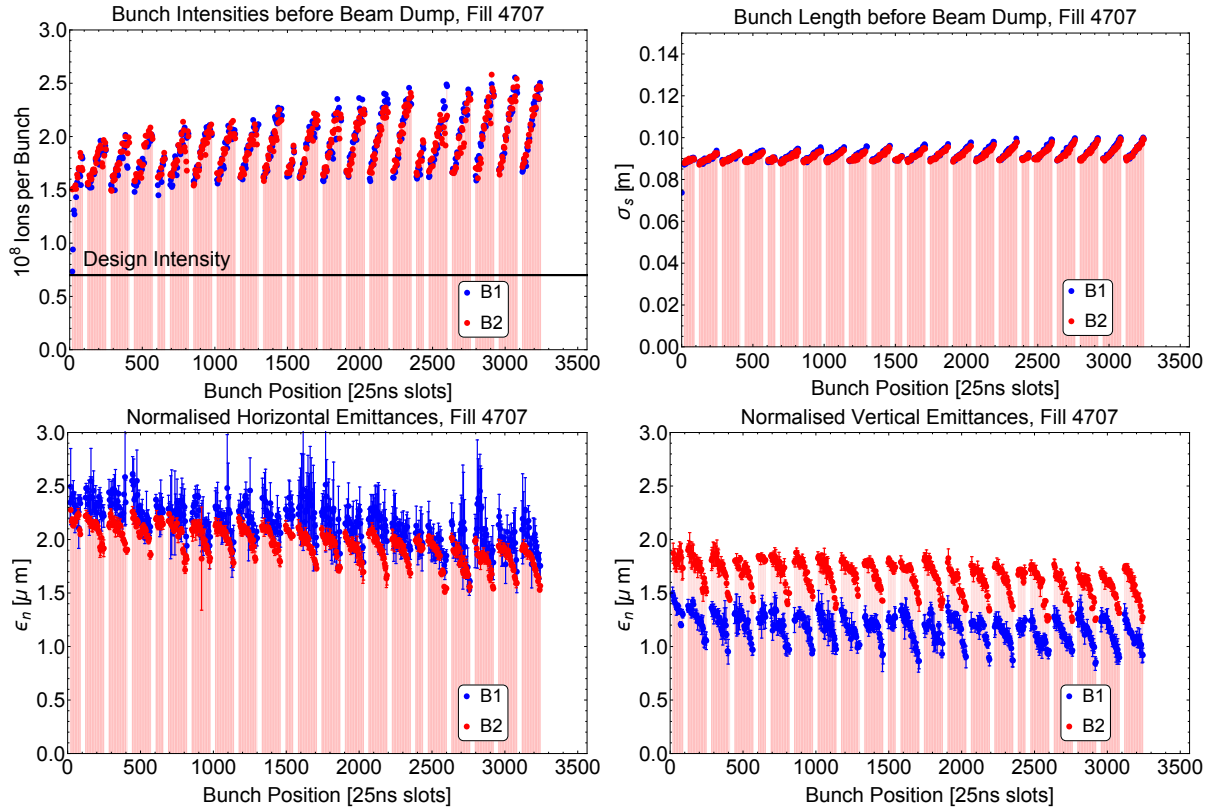


Figure 11: Beam parameters of Fill 4707 just before the beams were dumped. Top: bunch intensities (left), bunch length (right); Bottom: Emittances from BSRT, horizontal (left) and vertical (right). Blue displays Beam 1, red Beam 2. The error bars on the emittance show the statistical standard deviation over the last 3 measurements, the error on the β -function is not included.

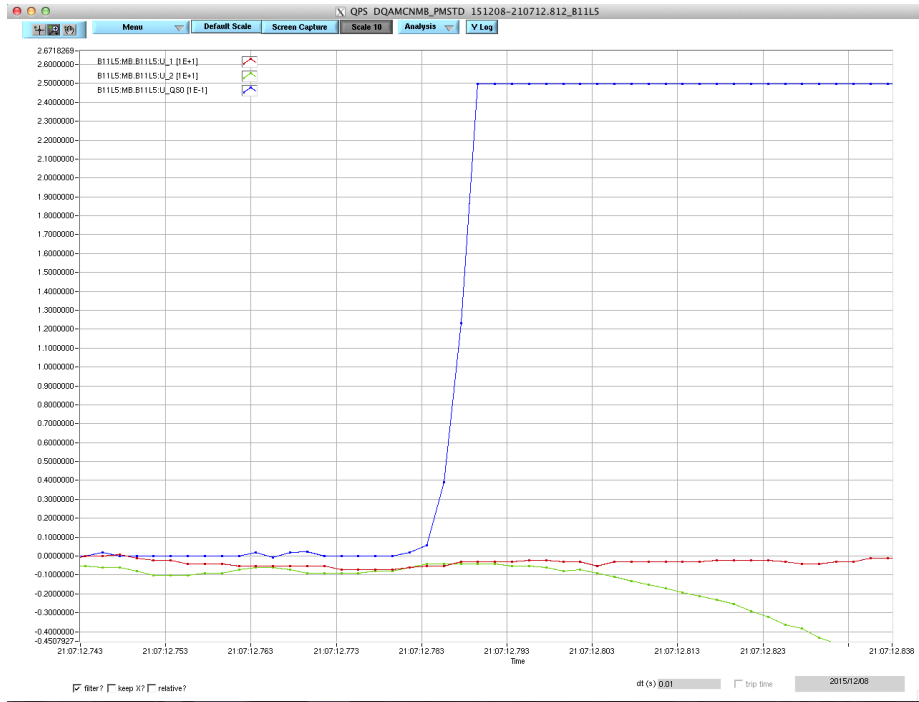


Figure 12: Quench detection. The measurement of the voltage difference across the two magnet apertures (blue line) shows a rise time over a few milliseconds, indicating a quench of one of the two apertures. Plot from Post Mortem Browser.

4 Preliminary analysis with FLUKA

FLUKA shower simulations were carried out to derive a first estimate of the peak power density in magnet coils during the quench test, therefore providing a first tentative estimate of the steady-state quench level of MB magnets at 6.37Z TeV. To verify the predictive ability of the simulation model, simulated BLM signals were compared against BLM measurements. The particle shower simulations were based on BFPP1 loss distributions derived with MAD-X, assuming a nominal beam screen aperture (23.25 mm) and an orbit bump of +0.5 mm like the one used during the quench test. As the actual loss location can differ by a few meters from the theoretical one (due to beam screen tolerances etc.), the loss location was adjusted in the FLUKA simulations in order to achieve the best match with the measured BLM signal pattern. The simulations indicated that the actual loss location differed by about 1 – 1.5 m from the MAD-X prediction.

A comparison between the measured BLM signals and the simulated ones can be found in Fig. 13. The measured signals were taken from Running Sum 9 (1.3 s integration time) slightly before the quench happened, i.e. when the orbit bump was adjusted to +0.5 mm and the luminosity was at its highest value of roughly $2.3 \times 10^{27} \text{ cm}^{-2}\text{s}^{-1}$ (around 3.74 h in time scale of Fig. 10). Simulated signals were normalized using the measured luminosity and assuming a BFPP1 cross section of 276 barn. In order to demonstrate the sensitivity of the BLM pattern to the impact location of the BFPP1 beam on the beam screen, the figure shows FLUKA results for two different loss locations differing by 50 cm. As can be seen in the plot, such a small shift visibly alters the ratio of BLM signals in the vicinity of the loss location. In general, a very good agreement between simulated and measured signals is achieved for an assumed loss location of 414.8 m left of IP5. The main disagreement is found for BLMs on the connection cryostat, what calls for

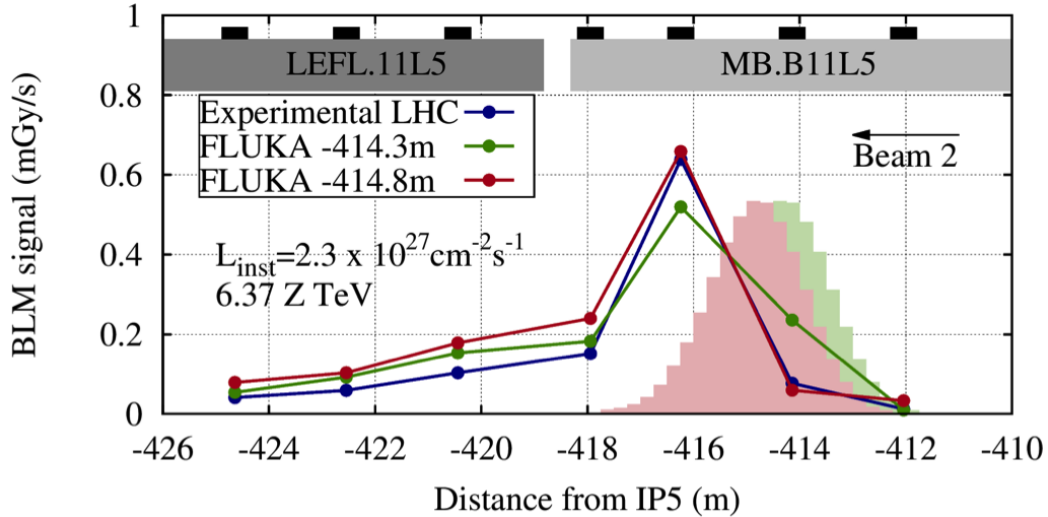


Figure 13: BLM signal comparison between experimental data from the quench test and FLUKA data assuming two different loss locations. The beam direction is from the right to the left. The statistical error of the simulated data is less than 12% for BLMs downstream of the impact locations. The position of the cryostat, dipole and BLMs is illustrated in the upper part of the plot. The particle distributions for the different loss locations assumed in the simulations are shown in the green and red histograms.

a more in depth sensitivity analysis. In addition, further studies are needed to investigate the potential displacement of the closed orbit with respect to the beam pipe, which gives rise to the observed discrepancies between theoretical and actual loss locations. The discrepancy appeared to be more pronounced for the orbit bump applied during regular fills than for the one applied during quench test.

In order to derive a first estimate of the peak power deposition in the MB.B11L5 coils, a cylindrical mesh was placed over the model of the dipole in FLUKA recording the energy deposited in the magnet coils in segments of $10 \text{ cm} \times 0.2 \text{ cm} \times 2 \text{ degrees}$ (z, R and Φ respectively in cylindrical coordinates). The simulation results were normalized in the same way as the BLM signals. Figure 14 presents the longitudinal distribution of the peak power density in the MB coils. The figure shows both, the peak power density at the inner edge of the cable and the radially averaged power density over the cable. The figure includes only the results for the most accurate loss location according to the previous BLM comparison (-414.8 m), but it is worth mentioning that contrary to the BLM pattern, the peak power in the coils is not affected by the position of the loss distribution. This can be justified because the energy is in any case deposited deep inside the dipole.

As the heat has enough time to spread across the cables' cross-section, one typically uses the radially averaged power density to quantify the quench level for steady-state losses. As can be seen in the figure, the maximum radially averaged power density is estimated to be around 15 mW/cm^3 , which is lower than previous predictions derived with QP3 [11] model calculations. As for the BLM pattern, these results should be considered preliminary in view of a subsequent sensitivity analysis. The peak power deposition in the coils depends strongly on the longitudinal and vertical spread of the impact distribution and hence more studies are needed to quantify the uncertainty of the above mentioned peak power density.

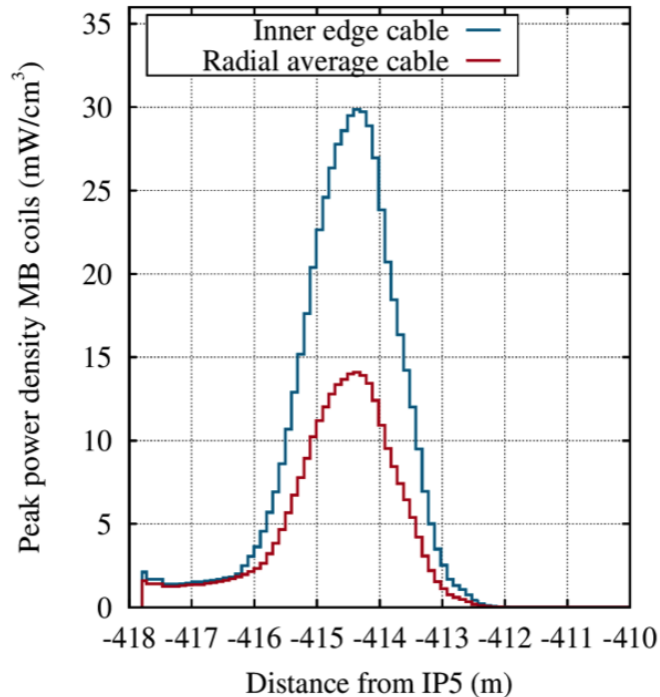


Figure 14: Peak power density in the MB.B11L5 coils during the quench test estimated by FLUKA simulations.

5 Summary and Conclusions

The experiment was a success. A beam-induced quench of the expected magnet MB.B11L5 occurred at 21:07 on 8 December 2015, induced by the loss of the BFPP1 ions created during luminosity production. The quench occurred at an instantaneous luminosity value of around $\mathcal{L} \approx 2.3 \times 10^{27} \text{ cm}^{-2}\text{s}^{-1}$ according to the CMS online luminosity publication. This corresponds to a peak power density in the coils of about 15 mW/cm^3 (from FLUKA simulations), assuming a BFPP1 cross-section of 276 b at 6.37 Z TeV beam energy (calculated with the expressions given in [10]).

From previous quench tests, which had never reached the appropriate regime, the steady state quench limit had been inferred to be higher [9].

The detailed analysis of the experiment including MADX, FLUKA and QP3 [11] simulations has already started. However, to obtain an accurate value of the steady-state energy deposition inducing a quench, more simulations are needed. In particular, the situation of the potentially displaced beam screen in the connection cryostat and MB.B11 left of IP5 has to be modelled in order to fit the FLUKA simulation to the observed BLM signals.

The experiment has shown that the orbit bumps introduced around IP1 and 5 were already required for quench mitigation in the 2015 Pb-Pb run and that they will be required in the future. The installation of special collimators in the dispersion suppressors to absorb the secondary beams around IP2 also appears necessary. The final results of this test are a crucial ingredient for the evaluation of the need of these collimators.

Acknowledgements

We thank the OP team on shift for setting up the beams and carrying out the experimental steps. We also acknowledge the BLM team for setting up the special BLM thresholds required for this experiment. We also thank L. Rossi for his encouragement.

References

- [1] R. Bruce, “Beam loss mechanisms in relativistic heavy-ion colliders”, CERN-THESIS-2010-030, ISRN:LUNTDX/NTMX1009SE.
- [2] R. Bruce, “Simulation of ion beam losses in LHC magnets”, CERN-THESIS-2005-053.
- [3] M. Schaumann, “Heavy-Ion Performance of the LHC and Future Colliders”, CERN-THESIS-2015-195, urn:nbn:de:hbz:82-rwth-2015-050284.
- [4] R. Bruce, S.S. Gilardoni, J.M. Jowett, “BFPP losses and quench limit for LHC magnets”, CERN-LHC-Project-Note-379.
- [5] A. Lechner et al., “BFPP losses in the connection cryostat: power deposition and dose estimates for Run 2 (and some outlook to HL-LHC)”, Presentation at the LHC Machine Committee on Sept. 2nd 2015. <http://indico.cern.ch/event/442208>
- [6] T.T. Bhlen, F. Cerutti, M.P.W. Chin, A. Fasso, A. Ferrari, P.G. Ortega, A. Mairani, P.R. Sala, G. Smirnov and V. Vlachoudis, “The FLUKA Code: Developments and Challenges for High Energy and Medical Applications”, Nuclear Data Sheets 120, 211-214 (2014).
- [7] A. Ferrari, P.R. Sala, A. Fasso, and J. Ranft, “FLUKA: a multi-particle transport code”, CERN-2005-10 (2005), INFN/TC_05/11, SLAC-R-773.
- [8] M. Kalliokoski, B. Auchmann et al., “BLM Thresholds for 2015 Ion Quench Tests”, LHC-BLM-ECR-0043, EDMS Doc. Nr 1564280.
- [9] B. Auchmann et al., “Testing beam-induced quench levels of LHC superconducting magnets”, PRSTAB 18, 061002 (2015).
- [10] H. Meier et al, “Bound - free electron-positron pair production in relativistic heavy - ion collisions”, Physical Review A, volume 63, 032713 (2001).
- [11] A. Verweij et al., ”QP3: Users Manual”, CERN, 2008.